The correlation of microchemical properties to antiwear (AW) performance in ashless thiophosphate oil additives

M.N. Najman[a], M. Kasrai[a,*], G. M. Bancroft[a], B.H. Frazer[b] and G. De Stasio[b]

[a]*Department of Chemistry, University of Western Ontario, London, Ontario, Canada N6A 5B7*
[b]*Department of Physics, University of Wisconsin-Madison, Madison, Wisconsin 53706, USA*

Received 7 March 2004; accepted 9 May 2004

X-ray absorption near-edge structure (XANES) spectroscopy at macro-scale (mm^2) and X-ray photoelectron emissions microscopy (X-PEEM) at micro-scale (μm^2) have been used to investigate the chemistry and spatial distributions of chemical species in tribochemical films generated from ashless thiophosphate oil additives on steel. Two different ashless thiophosphate additives were used: a triaryl monothiophosphate (MTP) and a dialkyldithiophosphate (DTP). Atomic force microscopy (AFM) and secondary electron microscopy (SEM) were also used to investigate the thickness and the topography of the tribofilms. Macro-scale XANES analysis showed that both ashless thiophosphates reacted with the steel surface to produce short to medium chain polyphosphates as the main constituent and sulfur species as minor component. From the PEEM experiment, it was found that the DTP tribofilm was microchemically heterogeneous, with areas of varying degrees of polyphosphate chain length. Conversely, MTP formed a tribofilm microchemically homogeneous, with areas comprised of only short chain polyphosphates. From, the different areas of polyphosphate chain length within the DTP tribofilm, colour-coded polyphosphate distribution map was generated. AFM, X-PEEM and SEM revealed that the DTP film was thicker and was composed of AW pads that were wider in area than MTP. This resulted in a smaller wear scar width (WSW) value for DTP. This is the first time that all these analytical techniques have been combined to better understand the nature of the tribofilms from ashless additives. We have concluded that an ideal AW film is comprised of a thick film with pad-like structures that are wider in area and microchemically heterogeneous, with areas of varying polyphosphate chain length.

KEY WORDS: thiophosphates, XANES spectroscopy, X-PEEM microscopy, anti-wear, AFM, wear protection

1. Introduction

In engine and other industrial lubricants, zinc dialkyldithiophosphates (ZDDPs) have been the additives of choice to provide protection against wear. In addition to the antiwear (AW) properties ZDDP provides to metal surfaces, ZDDPs possess antioxidant properties that are equally beneficial to the oil. Environmental implications of using ZDDP, however, have been addressed, and the necessity to use more environmentally friendly oil additives has become ever more apparent [1,2]. Consequently, this has forced oil suppliers to look for alternatives to ZDDP that are both ashless and contain reduced amounts of both phosphorus and sulfur. Ashless thiophosphates are a common replacement, and research on these of additives has increased considerably over the last 10 years. These additives have been shown to provide wear protection comparable to certain types of ZDDP's and in some cases outperforming them [3]. While many of the studies done on these additives have focussed primarily on their physical properties and AW performance, little or no emphasis has been placed on the chemistry of the rubbed surfaces. The interface between opposing rubbing surfaces is a complex system that involves both mechanical and chemical interactions and as a result, require the use of methods that yield topographical, elemental and chemical information about the nature of the surface at high spatial resolution [4].

X-ray absorption near edge structure (XANES) spectroscopy is an established surface analytical technique that can provide a wealth of chemical information on AW reaction films, in general [5–8]. Our group has utilized the XANES technique to provide unprecedented chemical information on both the phosphorus and sulfur chemistry of AW films generated from ZDDP [5,6]. Using both the total electron yield (TEY) and fluorescence yield (FY) modes of detection at the P and S L- and K-edges, simultaneous information can be obtained on both the near surface (TEY) and bulk chemical information of the films [9]. Recently, application of the XANES technique has been extended beyond the realm of ZDDP, to the study of ashless oil additives including a variety of organic compounds containing phosphorus and sulfur [7–8, 10]. Now while a plethora of information has been obtained on reaction films generated from a wide selection of oil additives, the analyzed area in both the

*To whom correspondence should be addressed.
E-mail: mkasrai@uwo.ca

L- and K-edge experiments are typically on the order of a few square millimeter, dimensions too large to provide any detailed chemical information on the antiwear "pads", which are usually microns in size [11].

Photoemission electron microscopy (PEEM) is a relatively new technique that has been developed extensively to utilize the high brightness of synchrotron light sources in order to obtain a sufficient signal at a high spatial resolution [12]. This soft X-ray spectromicroscopic technique images emitted electrons from a sample with tunable X-rays. The images are recorded at incremental photon energies in order to chemically distinguish different components of the system. As a result, XANES spectra of the absorbing atom can be obtained with the energy resolution given by the resolving power of the X-ray monochromator and the spatial resolution determined by the optics in the microscope [13].

PEEM has already been applied to the microchemical study of tribological samples. Anders *et al.* investigated the tribochemical interactions, at the sub-micron level, between the slider and the hard disk surface using PEEM [4]. It was revealed that during the wear process, the degraded perfluoropolyether (ZDOL) lubricant additive was transferred from the disk to the slider and accumulated in the scratches. Local C K-edge XANES spectra of the degraded lubricant revealed the formation of carboxylic bonds while the diamond-like carbon (CH_x) coating on the slider was completely removed. Sliders used in a wear test on unlubricated disks did not reveal the presence of any carboxylic bonds. Canning *et al.* [11] used a version of the PEEM technique called MEPHISTO (Microscope a Emission de Photoelectrons par Illumination Synchrotonique de Type Onduleur, i.e., photoelectron emission microscope by synchrotron undulator illumination) to elucidate the microchemical properties of AW films generated from ZDDP. Both secondary electron images and high quality X-ray absorption spectra were obtained, providing detailed information on both the chemistry and topography of the polyphosphate films. Very recently nanometer scale chemical and mechanical characterization of selected features of a tribologically derived zinc dialkyl-dithiophosphate (ZDDP) antiwear film have been reported [14]. Mechanical properties of antiwear pads were determined by imaging nanoindentation. The same features were studied by X-ray photoelectron emission microscopy (X-PEEM), which provides both elemental and chemical information at ~200 nm spatial resolution.

In this study, we have applied PEEM to study the chemical structure of AW films generated from ashless thiophosphate oil additives. More importantly, we compare the microchemistry of AW films generated from an aryl monothiphosphate and a dialkyldithosphate, in an attempts to correlating microchemical properties of these films to wear protection performance.

2. Experimental

Both oil additives and base stock solutions were supplied by Imperial Oil (Esso) Canada and were used without any further purification. Two different ashless thiophosphate additives were used. The first additive used was an ashless triaryl monothiophosphate and is referred to as MTP. The second additive used was an ashless dialkyldithiophosphate and is referred to as DTP. The lubricant formulation was achieved by dissolving the additive by weight in the low sulfur base stock. The concentrations used in this study were 0.5 wt.% DTP and 1.5 wt.% MTP, respectively. These concentrations were recommended by the suppliers. Chemical structures of the additives used in this study are shown in figure 1. A pin-on-flat Plint High Frequency wear tester was used to prepare the tribofilms. The oil solution containing the additives (~20 ml) and steel coupon (52100 steel) were both placed into the wear tester with the oil solution heated to a temperature of 100 °C. The cylindrical pin (52100 steel) was then loaded flat against the steel coupon with a force of approximately 220 N. The duration of the wear test was 1 h at a rubbing frequency of 25.0 Hz. Upon completion of the wear test, the coupon was gently rinsed in a light hydrocarbon solvent to remove any excess oil present on the surface. The wear scar width (WSW) values were measured on the cylindrical pin using a calibrated optical microscope. The reported WSW values correspond to at least 15 measurements made along the axis of the pin. All the films were made in duplicate.

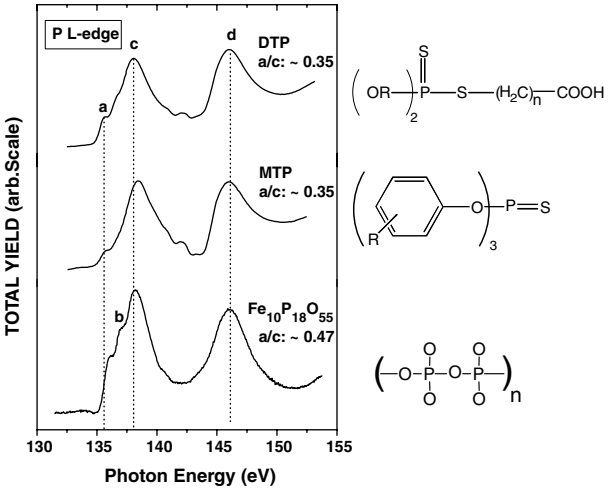

Figure 1. Conventional P L-edge XANES spectra (from ~5 mm^2) of tribofilms generated from DTP and MTP in total electron yield (TEY) mode as compared with an iron polyphosphate model compound.

All XANES experiments were conducted at the 1 GeV Aladdin storage ring, University of Wisconsin, Madison [15]. The Grasshopper beamline was used to obtain P and S L-edge macro-XANES analyses. The Grasshopper soft X-ray beamline covers an energy range of 70–900 eV with a photon resolution of <0.2 eV at both the P and S L-edge. For the P and S L-edge, the energy scale was calibrated using a typical zinc dialkyldithiophosphate (ZDDP) at 134.8 eV for P and 164.0 eV for S (the most intense peaks). XANES photoabsorption spectra were recorded using the total electron yield (TEY) method of detection for macrochemical surface characterization [16]. P K-edge intensities were used to obtain average film thickness measurements using methods described previously [17].

Soft X-ray spectromicroscopy experiments were performed using the SPHINX (Elmitec GmbH) photoemission electron microscope (X-PEEM), located on the 6 M toroidal grating monochromator (TGM) beamline [18]. The samples were rinsed in n-hexanes prior to entry into the vacuum chamber to remove any excess oil. Details of the PEEM experiment have been explained elsewhere [12]. Briefly, the incident X-ray beam is focused on the sample that is positioned at a grazing angle of 30 °. The size of the focused spot was set at 30 μm in width. The emitted photoelectrons are collected by a series of electrostatic lenses and imaged onto a phosphor screen that is then read by a CCD camera. In the SPHINX microscope, there is a combination of seven stigmators and deflectors and six magnetic lenses, which are used to focus and magnify the secondary electron image. The aperture in the microscope acts as an energy filter, allowing only low kinetic energy electrons to pass through and hence be imaged, thus making the technique surface sensitive. At low kinetic energies, 0–20 eV, the electron intensity is dominated by secondary electrons, which is a direct measure of the X-ray absorption coefficient of the sample as a function of photon energy [19]. For the actual acquisition of PEEM data, a "stack" of images of small regions is acquired at closely spaced intervals in X-ray energy [20]. In this PEEM study, a stack consisting of 301 images taken over an energy range of 130–160 eV with an energy spacing of ~ 0.1 eV for the P L-edge region; and 301 images taken between 160 and 190 eV for the S L-edge region. The resolution of the PEEM images was determined to be roughly 200 nm per pixel. After the images were aligned, the P and S L-edge XANES spectra of distinctive regions within the wear scar of both AW films were digitally extracted from the stack using *aXis 2000* software. *aXis 2000* is a program for analysis of the X-PEEM images and spectra [21].

The XPS analyses were carried out with a Kratos Axis Ultra spectrometer using monochromatized Al K_α X-rays. The survey spectra were obtained (160 eV pass energy) in hybrid mode and the analyzed area was ~700×300 μ in size. The spectra were processed using CasaXPS software and quantified using sensitivity factors supplied by Kratos. SEM and EDX analyses of the tribofilms were performed at Surface Science Western, located at the University of Western Ontario. The samples were examined with a Hitachi S-4500 field emission SEM equipped with an EDAX Phoenix light element energy dispersive X-ray (EDX) analysis system. EDX analysis is capable of detecting all elements above atomic number 5 and has a minimum detection limit of ~0.5 wt.% for most elements. For this work an electron beam voltage of 5 kV was used for imaging and EDX analysis. This low voltage was reasonably surface sensitive allowing imaging of the thin glassy wear pads and also analysis for the elements of interest.

All AFM topography images were collected in air using a Nanoscope IIIa equipped with a Multimode™ head (Digital Instruments, Santa Barbara, CA). The images of the tribochemical films were recorded in contact force mode with V-shaped silicon nitride cantilevers possessing a nominal spring constant of 0.12 N/m.

3. Results and discussion

3.1. Macrochemical analysis of tribochemical films

XANES, XPS and SEM/EDX data of the tribofilm surfaces are discussed first. XANES spectra at the P L-edge, acquired on the Grasshopper beamline, on both the DTP and MTP tribofilms in TEY modes are presented in figure 1, along with an Fe(II) polyphosphate glass. The spectra are characteristic of typical P L-edge XANES spectra for phosphates. The general features for P L-edge XANES spectra have been explained elsewhere [22]. The intensity of peak *a* relative to peak *c* in P L-edge XANES spectra of polyphosphates, are known to correlate well with the length of the polyphosphate chain [23]. Looking at the *a*/*c* ratios for both tribochemical films, the films appear to be mainly comprised of short chain polyphosphates at the near surface of the film (TEY). However, since the analyzed area in a conventional XANES experiment at the P L-edge is on the order of several square millimeter, the chemical properties obtained provide a macrochemical assessment.

Low resolution XPS survey scans were also performed on the wear scars of both tribofilm samples in order to provide a quantitative, elemental, near-surface analysis of the films. The results are presented in table 1. The spot size of the beam was 600 μ and XPS was performed on nine different regions within each wear scar, providing an overall average of the elemental distribution. As can be seen from the data, more phosphorus is present on the surface of the DTP tribofilm than for MTP, surprising since the concentration of the oil formulation for DTP was only 0.5 wt.%

Table 1.
XPS semi-quantitative analysis of ashless thiophosphate tribofilms.

		C1s	O1s	S2p	P2s	Fe3p	Zn2p
Energy Pos. (eV)		285.4	531.8	170.6	190.9	55.8	1022.5
Elemental composition (%)	MTP	49.0	33.2	1.0	6.5	6.4	0.84
	DTP	49.8	31.6	0.65	9.2	0.82	2.9

compared to 1.5 wt.% for MTP. The level of sulfur in both tribofilms appears to be only present in minute amounts and significantly less than phosphorus. For both tribofilms, carbon is detected at relatively high concentrations and can be attributed to the large amount of carbon present in both additives and the base stock solution in addition to the possibility of carbon contamination from the vacuum chamber during the XPS analyses. Even more surprising is the presence of zinc in the XPS spectra, especially since no zinc is present in either thiophosphate molecules. An explanation into the presence of zinc on the surface of the tribofilms will be addressed later on in this section.

SEM in combination with energy-dispersive X-ray analysis was used in the preliminary assessment of the topographical features of the tribofilm surfaces. Figures 2 and 3 clearly show that the DTP and MTP tribofilm surfaces are quite different from another. More detail into the morphology and topography of the films will be discussed in the PEEM section of this study. SEM also reveals that the tribofilms formed, in both cases, are not covering the entire steel surface homogeneously. This has also been seen in the formation of ZDDP tribofilms [24]. Both films have areas within the scar that are comprised of glassy pads; in between the glassy pads are areas of what appears to be steel substrate. EDX analysis confirms the observations from the SEM data. EDX spectra were obtained from points taken directly on the pad-like features and in between them for both tribofilms. The elemental chemistry is clearly different upon going from "on" the pad to "off" the pad. In both tribofilms, EDX revealed that there is a higher concentration of both phosphorus and oxygen on the glassy pads, while between the pads, both carbon and iron are present at higher concentrations. Interestingly, zinc is also present in the EDX spectra, especially in the case of the DTP film. In order to investigate the origin of zinc in the film, oil solutions were analysed by inductively coupled plasma emission spectrometry [25].

3.2. Elemental analysis of used oil by ICPES

MTP and DTP oil blends with and without ZDDP were analysed by ICPES after tribofilm formation. The results are shown in table 2. Concentrations of zinc and phosphorus measured in oil blends A and B are

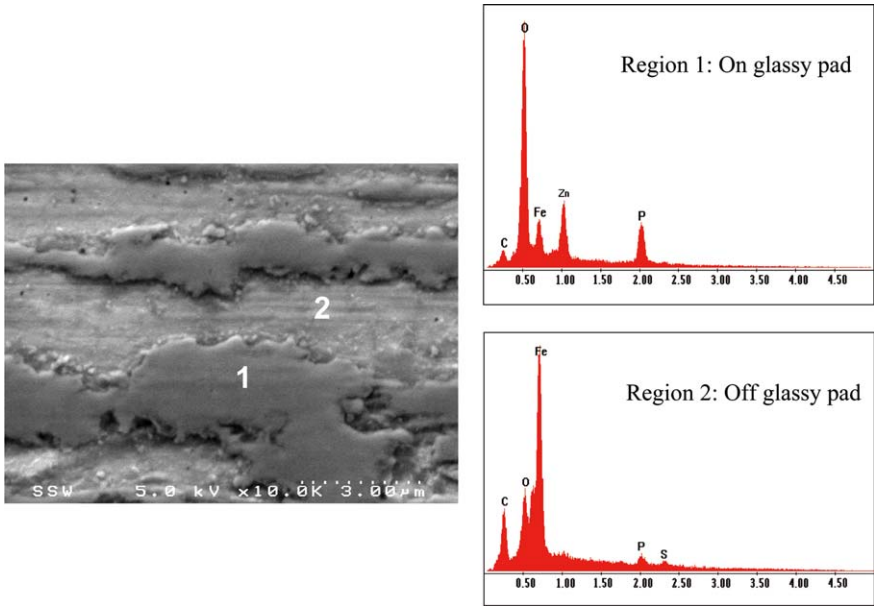

Figure 2. Scanning electron microscope (SEM) image and energy-dispersive X-ray (EDX) spectra of DTP tribofilm. EDX spectra was taken "on" and "off" the glassy pads.

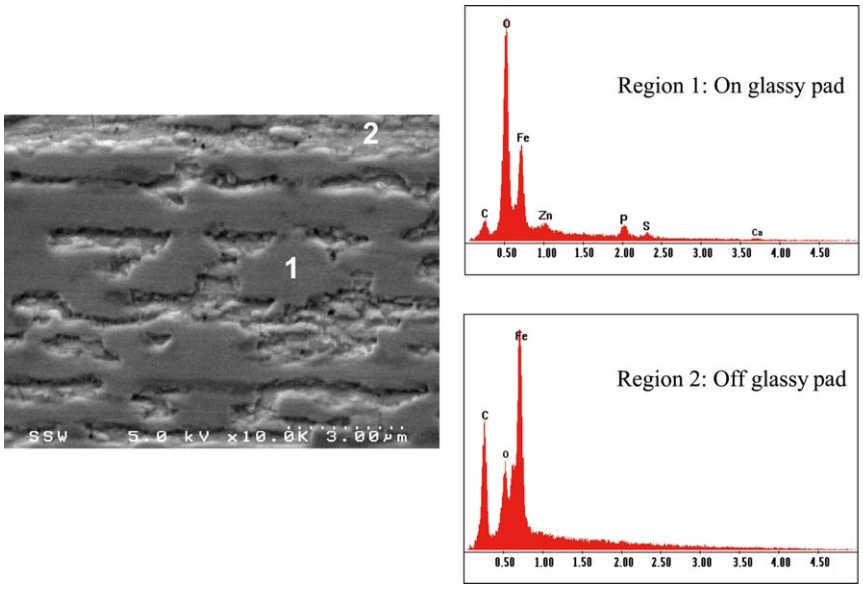

Figure 3. Scanning electron microscope (SEM) image and energy-dispersive X-ray (EDX) spectra of MTP tribofilm. EDX spectra was taken "on" and "off" the glassy pads.

Table 2.
Elemental concentration of oil solution measured by ICPES.

	Oil blends*	Iron (ppm)	Phosphorus (ppm)	Zinc (ppm)
A	1200 ppm ZDDP	2	1010	1040
B	1%DTP + 20 ppm ZDDP	< 1	914	16.9
C	1% MTP	3.5	423	1.2
D	1.5% MTP	5.5	661	< 1
E	0.5% DTP	< 1	479	1.6
F	1% DTP	< 1	917	2.4

*Oil blends were analysed after AW films were made.

very close to what is expected from the original ZDDP concentrations in the blends. However, there is small amount of zinc present in oil blends C–F, which is not expected. The mount of zinc for the MTP oil blends is less than those of DTP blends. Zinc can originate from different sources in the Plint machine. The obvious source, which was discovered later, was a copper–zinc drainage plug located in the basin of the Plint machine. DTP being a dialkyldithiophosphate molecule with a terminal carboxylic acid group (TAN = 165) can react with the plug at 100 °C to form zinc phosphate. This was replaced with a steel plug. However, in spite of through cleaning and sonicating all parts of the oil containers and rubbing arm which comes in contact with the film in hexane, zinc could not be totally eliminated from the film. There is always small zinc in films as measured by XPS or EDX. Due to years of using ZDDP in our Plint machine, it seems small amount of ZDDP is trapped in the walls of the oil container, which is released during the film formation. It is also possible that the steel used contains small amount of zinc. We are in the process of replacing all those parts. At this point, we do not believe such a small amount of zinc has any significant effects on the chemical nature of the tribofilms discussed below.

3.2. Microchemical analysis of tribochemical films

3.2.1. Nature of local polyphosphate chain length within wear scar

The general topographical features of both tribofilms are displayed in figure 4. As seen with both PEEM and AFM, it is clearly evident that the tribofilms formed are different from one another. Looking first at DTP, the 120×120 μm AFM image reveals that the surface of the tribofilm is quite heterogeneous, with the pads elongated and oriented in the sliding direction. The film is composed of somewhat larger pads, with diameters between 2.5 and 5.0 μm as determined from the PEEM image. Although indentation studies have yet to be performed on ashless thiophosphate AW films, indentation studies on AW films generated from alkyl ZDDP showed that larger pads

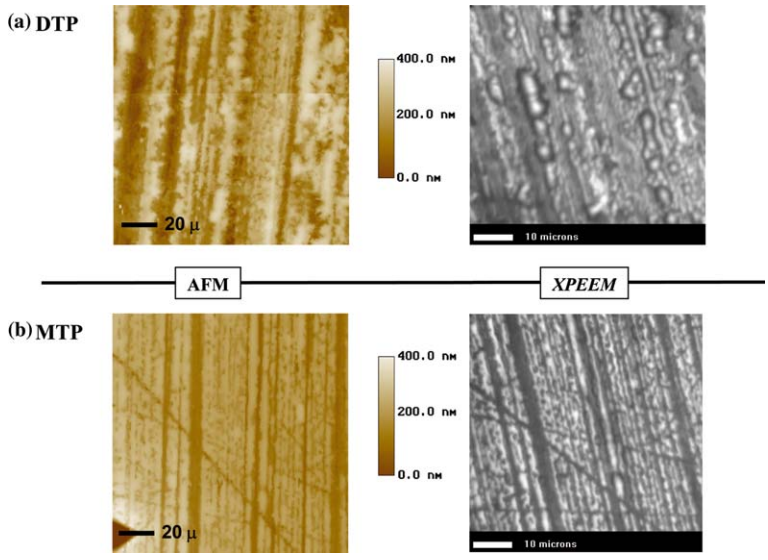

Figure 4. Height mode atomic force microscope images compared to topographical PEEM image for the two AW films prepared.

where shown to possess a very high indentation modulus, a significant resistance to plastic flow in addition to carrying the load during wear testing [26]. Certainly in our study on the tribological properties of organosulfur EP additives [8], the formation of smaller pads was also associated with poor wear protection performance.

Looking at the MTP tribofilm (figure 4(b)), AFM shows that the heights of the pads appear to be less than the pads formed by DTP. The pads are quite homogeneous in morphology, and are composed of thin, elongated pads oriented in the sliding direction. The pad widths in the MTP AW film were in the range of 1.5–2.0 μm, on average, somewhat narrower than the DTP pads.

Figure 5 shows a PEEM images revealing the topography and spatial distribution of phosphate in the tribofilm generated from DTP. The phosphate distribution was obtained the following way. An image was first acquired at a photon energy below the phosphorus L absorption edge (133.1 eV), (figure 5(a)). Obtaining an image below the absorption edge of P reveals mainly topographical contrast. Next, another image was taken at the phosphorus L absorption edge (137.2 eV). The image shown in figure 5(b), is the subtraction of these two images showing mainly chemical/elemental contrast. Looking at the ''difference images'', as the photon energy approaches the absorption edge (not shown), one can actually see the image intensity of the pad-like structures begin to increase, eventually reaching a maximum intensity at the absorption edge.

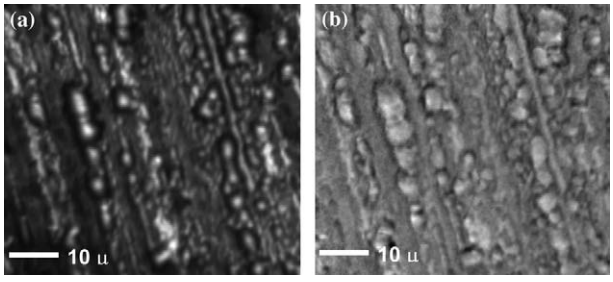

Figure 5. PEEM images of area of tribochemical film generated from the DTP additive. Image (a) is taken at a photon energy of 133.1 eV (showing contrast mainly due to topography). Image (b) is a subtraction of image (a) from an image acquired at 137.2 eV (showing contrast due to topography and the presence of phosphorus on the surface of the tribofilm).

Our main goal of this study was to examine the microchemistry of an AW film to determine if there were variations in the polyphosphate chain length. Conventional XANES spectroscopy at the P L-edge yields an analyzed area on the order of several square millimeter in area, dimensions too large to provide any microchemical information. Using PEEM, however, local XANES spectra can be obtained for much smaller area (μm^2). A series of images are taken as a function of energy, the spectra can then be digitally extracted with a spatial resolution dictated by the resolution of the microscope and the energy resolution governed by the resolution of the monochromator. It was determined that each pixel in the PEEM image from the SPHINX microscope is roughly 0.04 μm^2, an area more than sufficient to conduct microchemical analyses.

Figure 6 shows a PEEM image of an area where local XANES spectra at the P L-edge were taken within the wear scar for a DTP AW film. XANES spectra were extracted from several areas within this PEEM image as indicated by the labelled areas. Several regions were examined to determine if in fact there were differences in polyphosphate chain length from pad to pad. As mentioned earlier in this article, the intensity of peaks *a* and *b* relative peak *c* correlate

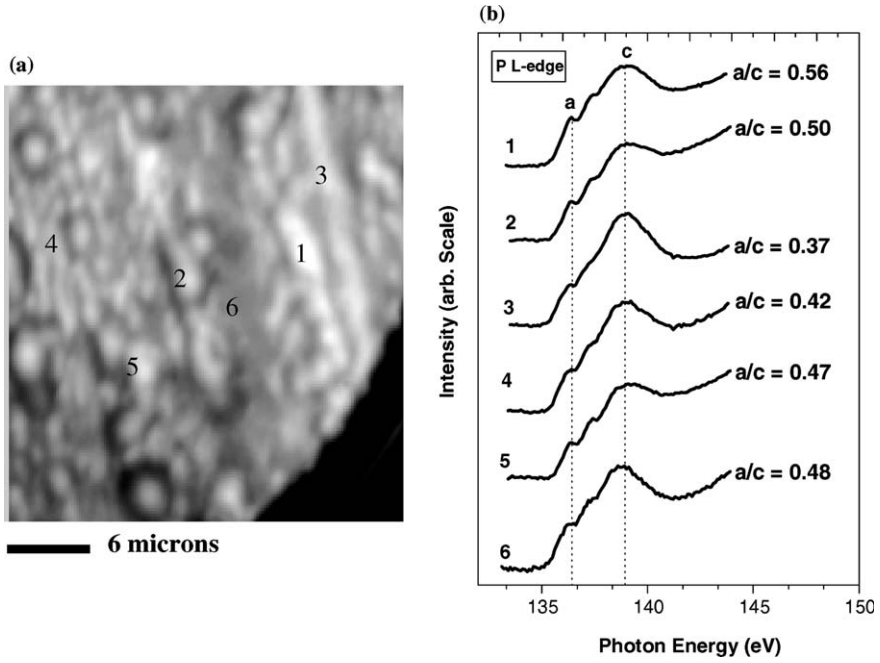

Figure 6. Detailed microchemical analysis of a region within the wear scar of AW film of DTP. (a) PEEM image with labeled areas indicating where local P L-edge XANES spectra were extracted. (b) Corresponding P L-edge.

very well to polyphosphate chain length, i.e., a higher ratio of a/c suggests longer chain polyphosphates. With this in mind, the a/c ratios of the areas analyzed are shown beside the corresponding P L-edge spectra, 1–6, respectively. Now while the P L-edge local XANES spectra of the different regions all look similar to one another, there are variations in the ratio of a/c. From looking at these ratios, it is clear that there are variations in the microchemical properties of the DTP film, with local areas consisting of varying degrees of polyphosphate chain length. It is only in the mico-scale analysis that we find this variations.

For the MTP AW film, the same pattern is not observed. As can be seen in figure 7 for a section of

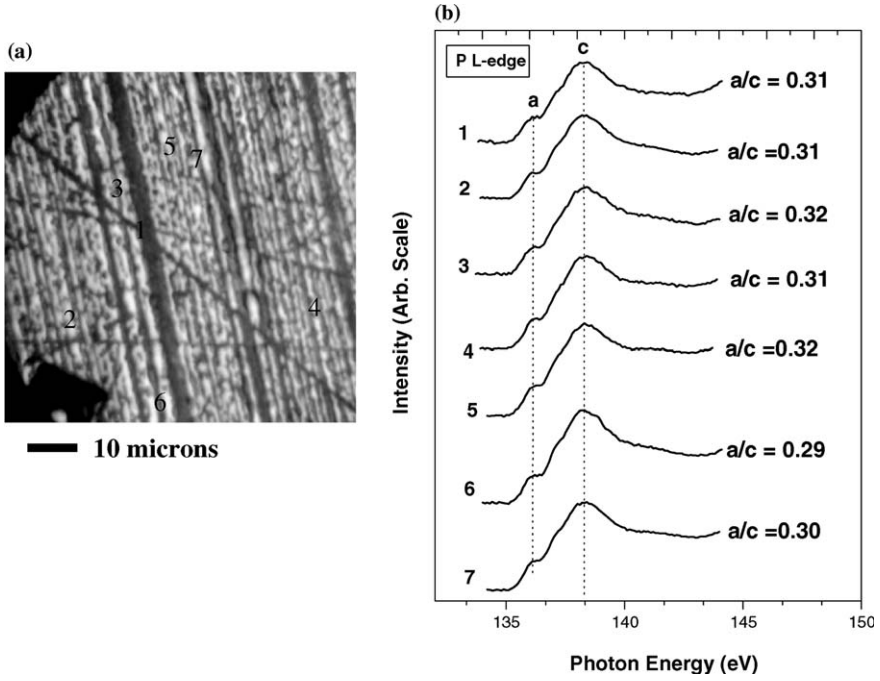

Figure 7. Detailed microchemical analysis of a region within the wear scar for AW film of MTP. (a) PEEM image with labeled areas indicating where local P L-edge XANES spectra were extracted. (b) Corresponding P L-edge XANES spectra.

the MTP AW film, the extracted spectra taken from the corresponding PEEM image reveals microchemical homogeneity throughout the analyzed area of the film. Looking at the a/c ratios of figure 7(b), there is little or no change in the a/c ratio across individual pads. Several different areas were also investigated (not shown) with similar results, thus concluding the AW pads that are formed during tribofilm formation are predominantly or almost completely short chain polyphosphates. It is also of interest to note that conventional XANES revealed that macrochemically, the polyphosphate chain length between the two AW films were similar (see figure 1).

3.2.2. *Derived semi-quantitative component maps of DTP tribofilm*

Thus far, we have shown that local XANES spectra on the sub-micron level obtained through PEEM can be used to discriminate areas of different polyphosphate chain lengths within an AW film. The two different types of spectra observed, which vary on the basis of intensity ratio of peaks *a–c*, can be used as individual components to obtain a distribution map from the set of PEEM images. Details of the quantitative analysis have been presented elsewhere [27], however, this method has been established with much success and has been applied to a range of materials including polymers and proteins [20,27,28]. Briefly, a linear regression analysis was applied pixel-by-pixel to the acquired image sequence in order to derive the component maps. This allows for full spectral variation to be used in deriving the maps. Since the tribofilms studied are not comprised of one pure component but rather a mixture, no quantitative reference standards exist, thus making the analysis semi-quantitative [27].

Figure 8 displays the systematic derivation of a spatial distribution map of polyphosphate chain length for the AW film of DTP. Figure 8(a) shows the different regions within the AW film where the P L-edge spectra were extracted and the a/c values determined. After a spline background was removed from the raw P-L-edge XANES spectra, the spectra depicting areas of longer and shorter chain polyphosphates were used as individual components to generate the chemical map. The individual components are shown in figure 8(c). The bright, more intense areas, reveal concentrated areas of shorter and longer chain polyphosphate, for each component, respectively. Figure 8(d), is the resulting color-coded chemical map after combining the individual components of figure-8(c). The P 2p spectromicroscopy reveals that there are areas of long chain polyphosphates that are segregated from areas of shorter chain polyphosphates. Upon closer inspection of figure 8(d), there are areas where

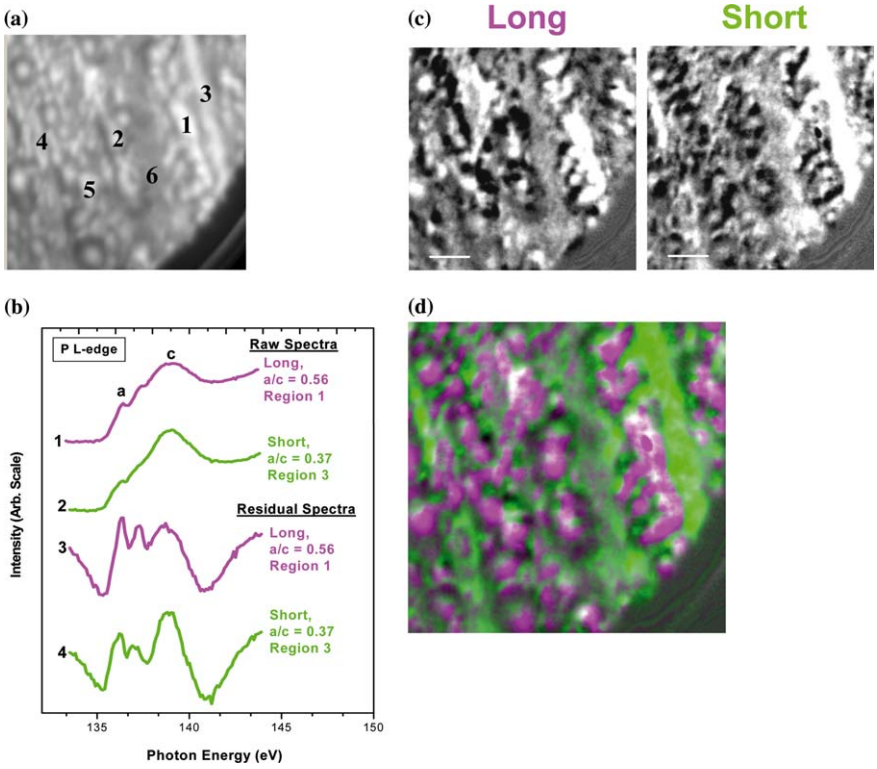

Figure 8. Chemical mapping of polyphosphate chain length distribution of AW film generated from DTP. (a) Topographical PEEM image of selected regions of interest. (b) P L-edge XANES spectra (raw) of regions 1 and 3 in figure 6–6a. Spectra 3,4 correspond to residual P L-edge XANES spectra of regions 1 and 3 after a spline background was removed. (c) Derived quantitative chemical maps of the two components used. Spectra 3 and 4 were used to drive the components maps. (d) Color-coded composite map displaying polyphosphate chain length distribution. Longer chain polyphosphates are colored in mageneta and green depicts shorter chain polyphosphates.

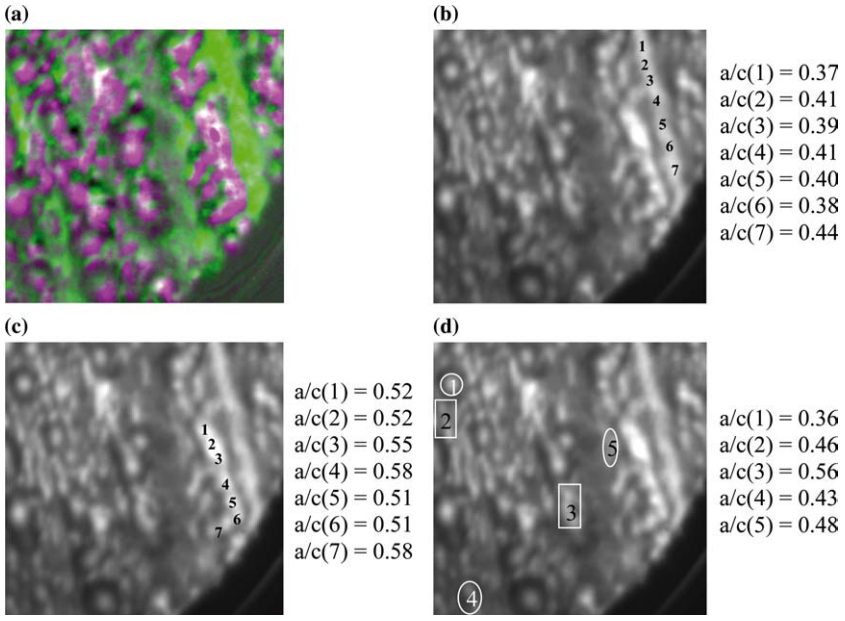

Figure 9. Selected regions to determine consistency between distribution map and actual areas of different polyphosphate chain length. All a/c values are consistent with distribution map in 6–9a.

both long and short chain polyphosphate areas coexist, although, there appears to be a higher concentration of shorter chain polyphosphate within the area analyzed; results consistent with the macro-XANES analysis.

Since the varying intensity of the a/c ratios in the P L-edge XANES spectra obtained from the PEEM analysis was the basis for deriving the component maps for DTP, the procedure could not be performed for MTP due to microchemical homogeneity throughout the AW film.

The consistency of the color-coded map was evaluated in figure 9. The a/c values of 19 different areas were selected and tested against the map to determine its validity. Typically, using an internal standard method by which XANES spectra are extracted from the same image sequence is the best way of determining the accuracy and validity of the semi-quantitative analysis [27]. Figures 9(b) and (c) reveal 14 different spots where P L-edge XANES spectra were extracted along areas where the map revealed areas of short and long chain polyphosphate and a/c values tabulated. The 14 regions selected where XANES spectra were taken were roughly 0.04 μm^2. The microchemistry along both a longer chain and shorter chain pad remains relatively constant. The a/c values in all 14 cases are consistent with the map. As with figure 9(d), five selected regions were evaluated and the a/c values extracted for these regions are in good agreement with the map as well. This entire process was used to investigate several other regions within this wear scar (not shown) and the results were also consistent with the distribution maps that were generated.

3.2.3. Distribution and chemical nature of sulfur within wear scar

In addition to the microchemical nature of phosphorus in the AW films, the microchemistry of sulfur was also investigated. Figure 10 displays PEEM images taken at 172.1 eV, for the tribochemical films of both DTP and MTP, corresponding to the absorption edge of sulfur (172.1 eV for sulphate). S L-edge, spatially resolved, XANES spectra are shown for the regions selected. For DTP, the selected regions with high contrast yielded very noisy spectra, signifying very little sulfur present. This also confirms that the tribochemical films are dominated by the presence of phosphorus and that the contrast observed for images taken around the S L-edge is dominated by topography.

S L-edge spectra were also extracted from selected regions of the MTP AW film and appears that sulfur is in the form of iron sulfate. It is interesting to note that the P L-edge XANES spectra were also extracted from those exact areas indicating that both iron sulfate and iron phosphate co-exist at the same areas within the wear scar for MTP. However, since reasonable S L-edge XANES spectra were obtained from such large areas and could not be obtained from point extraction, as in the case for phosphorus, the amount of sulfur within the wear scar, relative to phosphorus is quite low, results that correlate well with XPS data described earlier in this study.

3.3. Correlation of microchemical analyses to wear protection

A summary of the tribofilm properties from each additive is displayed in table 3. Inspecting the data of

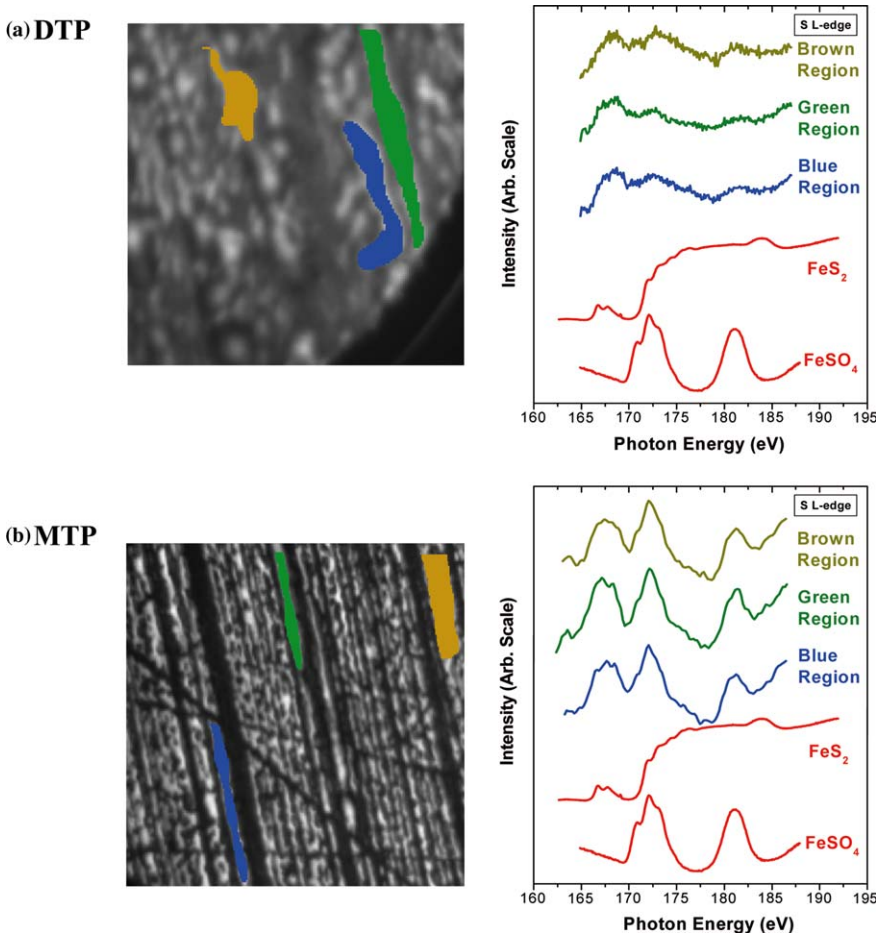

Figure 10. PEEM images taken at the absorption edge of sulfur for tribochemical films generated from both DTP and MTP, respectively, along with corresponding spatially resolved S L-edge XANES spectra.

Table 3.
A summary of the various quantitative properties experimentally determined for the tribochemical films generated from DTP and MTP, respectively. The chain length of the pads is determined by the relative intensity of peak *a* to peak *c*. The values given are an intensity ratio of the two peaks i.e., higher ratio value implies areas longer chain polyphosphate film.

Property	DTP	MTP
Wear scar width (WSW)	184 ± 14	230 ± 25
Film thickness (Å)	820 ± 10	570 ± 10
Average width of AW pads	2.5–5.0 μ	1.5–2.0 μ
Chain length of pads (intensity ratio of a/c)	0.37–0.56	0.29–0.32

table 3, it is clear these additives do behave tribochemically different. DTP provides significantly better wear protection than MTP as indicated by the smaller wear scar width (WSW) value. The better performance of DTP can be attributed to the formation of a thicker polyphosphate glassy, consisting of areas of longer chain length and possessing individual pad-like structure of greater width. However, how does each property affect the overall results?

Looking at film thickness first, DTP forms a relatively thicker film than MTP but in the past we have shown that film thickness is not necessarily the defining factor in determining wear protection. In some occurrences, the rate at which the additive decomposes at certain temperatures and begins to react with the metallic surface determines to some extent wear protection [8]. Previously in another study, we found that after 5 min. of wear testing, MTP provided better wear protection, on average, than DTP, even though DTP formed a thicker film [29].

The average width of the AW pads may also help to explain the WSW values. Both additives are able to generate thick pad-like structures oriented in the sliding direction. However, the average width of the pads generated is larger for DTP. The formation of larger pads may serve a double purpose in the wear protection process. First and more apparently, thick films of larger widths probably support more of the load during testing, resulting in less removal of material and thus better wear protection. This can also be seen in the SEM images present for both AW films. The DTP pads appear to have a concavity associated

with them whereas the MTP pads appear to have flatter features, a possible indication that pads are not supporting the applied load efficiently. In addition to this, if the pads are larger and take up more of an area, within the wear scar, there is less of a likelihood that an asperity will come into contact with an asperity on the opposing surface; statistically an asperity from the rubbing pin would most likely come into contact with a larger pad.

A similar study comparing the microchemical properties of AW films generated from aryl and alkyl ZDDPs [11] using soft X-ray spectromicroscopy was performed by Canning *et al*. Although the analyzed areas in their PEEM study were of larger dimensions than achieved here, similar results were found. The aryl ZDDP spectra and the morphology of the AW film were quite different than for the alkyl ZDDP. The alkyl ZDDP film contained a range of smaller and larger polyphosphate pads while the aryl ZDDP film consisted of mainly smaller, short chain polyphosphate pads. The authors attributed all of their findings to the rate of decomposition of the additive, with the aryl ZDDP not breaking down as quickly as the alkyl ZDDP, resulting in higher wear with aryl ZDDP. Previous studies have also shown aryl ZDDPs to break down more slowly than alkyl ZDDPs resulting in greater wear to the metal [30,31]. It was also reported that the smaller pads were composed of short chain polyphosphates while the larger pads were composed of longer chain polyphosphates. Now while their correlation of pad size to polyphosphate chain length was not conclusive in this study, there are striking similarities between the size of the pads and wear protection.

X-PEEM, in conjunction with some of the other surface analytical techniques used, has yielded some interesting findings in the attempt to correlate wear protection to both microchemical and micro-topographical properties of AW films. At the same time, however, intriguing and complex questions can also be raised. For instance, why is there such a variation in the size of the pads between the two additives? Are wider pads more mechanically durable than shorter pads in AW films? More importantly, what are the mechanistic features and underlying factors that determine the formation of wider AW pads? DTP, having a carboxylic acid group, is expected to react with iron oxide on the surface more readily than the neutral additive, MTP. As a result, nucleation of the polyphosphate structure starts at an earlier stage of rubbing, initiating pad growth earlier for DTP, ultimately resulting in larger pad growth. More work is needed to determine what factors affect the size of the pads formed during tribofilm formation since the size of the pads appears to have an impact on the antiwear efficiency of the additive. Future nanoindentation studies may also help to shed some light on how mechanically durable the pads are that have been formed under the tribochemical process.

In addition to the size of the pads having a role in wear protection, PEEM has also revealed that overall chain length of the pads may also have an effect as well. Referring back to table 3, DTP not only forms larger pads than its counterpart, but there are areas of longer chain polyphosphates within the AW film. MTP formed an AW film that was predominantly shorter in chain length. As mentioned earlier, Graham *et al*. concluded from their study of the nanomechanical properties of AW films generated from ZDDP, that the larger pads were associated with better wear protection [26]. This was due to their increased hardness as indicated by very high indentation moduli, a greater resistance to plastic flow and ability to carry a larger load during wear testing. Unfortunately, no correlation between the nanomechanical and microchemical properties (id. the polyphosphate chain length) of the films was investigated at that time.

From looking at the differences in polyphosphate chain length from sample to sample, an obvious question that can also be raised is why does DTP generate an AW film with pads of varying chain length as opposed to MTP, which forms an AW film with pads of uniform chain length? Furthermore, why are the pads for the MTP film substantially shorter in chain length than the pads for DTP? Ever more apparent is that since zinc was found in both the near-surface and bulk of the film for DTP, does the incorporation of zinc into the film play any added role in protecting a surface from wear. Because the surface analytical techniques used in previous studies of lubricant additives, in general, provide macro-chemical analyses, the above questions have never been addressed. This study has opened the door to a complex and fascinating new world into the analysis of tribochemically-derived samples for ashless thiophosphates.

4. Conclusion

In this study we have shown that the combination of XANES and PEEM are useful techniques for studying the chemical properties of AW films generated from ashless thiophosphate oil additives at the submicron level. Because the PEEM technique allows for the acquisition of a stack of images investigation of these properties at the submicron level, spatially resolved local XANES spectra can be obtained at sub-micron levels. Comparison between the reactivity of mono and dithiophosphates on steel under AW conditions was investigated at the micro-scale using soft X-ray spectromicroscopy at the phosphorus and sulfur L-edge. The following conclusions can be drawn from the results:

1. Macro-scale analysis of the tribofilms showed that both additives reacted under rubbing conditions to generate shorter chain polyphosphate films. XPS was used for quantification of the surface. The DTP tribofilm was comprised of more phosphorus than MTP.
2. From the PEEM experiments, it was found that the DTP tribofilm was microchemically heterogeneous, with areas of varying degrees of polyphosphate chain length. Conversely, MTP formed a microchemically homogeneous tribofilm, with areas comprised of only short chain polyphosphates.
3. For DTP, the different areas of polyphosphate chain length within the tribofilm, were used as individual components to generate a colour-coded polyphosphate distribution map for the area analyzed under PEEM. The accuracy and consistency of the distribution map was evaluated through measuring of the a/c ratios of the P L-edge XANES spectra from several different areas located within the area where the map was generated. In all cases, the a/c results were consistent with the generated map.
4. AFM and PEEM revealed that the DTP film was thicker and was composed of AW pads that were wider in area than MTP. This resulted in a smaller WSW value for DTP. We have concluded that an ideal AW film is comprised of a thick film with pad-like structures that are wider in area and microchemically heterogeneous, with areas of varying polyphosphate chain length.

Acknowledgments

This work was financially supported by Imperial Oil (Esso) of Canada, the National Research Council of Canada (NRC), and the Natural Science and Engineering Research Council of Canada (NSERC). We would like to thank Ross Davidson, Surface Science Western, for his assistance with the XPS and SEM/EDX data acquisition. The authors are also grateful to Drs. Kim H. Tan, Yongfeng Hu and Astrid Jürgensen, from CSRF and to the staff of the Synchrotron Radiation Center (SRC), University of Wisconsin, Madison, for their technical support and the National Science Foundation (NSF) for supporting the SRC under Award #DMR-0084402.

References

[1] R. Sarin, V. Martin, D.K. Tuli, M.M. Rai and A.K. Bhatnagar, Lub. Eng. 53 (1997) 21.
[2] W.A. Gehrmann, SAE Paper No. 921736 (1992)
[3] R. Sarin, A.K. Gupta, D.K. Tuli, A.S. Verma, M.M. Rai and A.K. Bhatnagar, Trib. Int. 26 (1993) 389.
[4] S. Anders, T. Stammler, W. Fong, D.B. Bogy, C.S. Bhatia and J. Stöhr, J. Vac. Sci. Technol. A. 17 (1999) 2731.
[5] Z. Yin, M. Kasrai, M. Fuller, G.M. Bancroft, K. Fyfe and K.H. Tan, Wear 202 (1997) 172.
[6] M. Kasrai, J.N. Cutler, K. Gore, G. Canning, G.M. Bancroft and K.H. Tan, Tribol. Transact. 49 (1998) 69.
[7] M.N. Najman, M. Kasrai, G.M. Bancroft and A. Miller, Trib. Lett. 13 (2002) 209.
[8] M.N. Najman, M. Kasrai and G.M. Bancroft, Trib. Lett. 14 (2003) 225.
[9] M. Kasrai, W. Lennard, R.W. Brunner, G.M. Bancroft, J.A. Bardwell and K.H. Tan, Appl. Surf. Sci. 99 (1996) 303.
[10] M.N. Najman, M.Kasrai and G.M. Baner of wear (in press).
[11] G.W. Canning, M.L. Suominen-Fuller, G.M. Bancroft, M. Kasrai, J.N. Cutler, G. De Stasio and B. Gilbert, Trib. Lett. 6 (1999) 159.
[12] T. Warwick *et al.*, Synchrotron Radiat. News 11 (1998) 5.
[13] J. Stöhr and S. Anders, IBM J. Res. Develop. 44 (2000) 535.
[14] M.A. Nicholls, P.R. Norton, G.M. Bancroft, M. Kasrai, T. Do, B.H. Frazer, G. De Stasio, Trib. Lett. 17 (2004) 205.
[15] G.M. Bancroft, Can. Chem. News 44 (1992) 15.
[16] M. Kasrai, Z. Yin, G.M. Bancroft and K.H. Tan, J. Vac. Sci. Technol. A 11 (1993) 2694.
[17] M. Fuller, L.R. Fernandez, G.R. Massoumi, W.N. Lennard, M. Kasrai and G.M. Bancroft, Trib. Lett. 8 (2000) 187.
[18] G. De Stasio *et al.*, Rev. Sci. Inst. 69 (1998) 3106.
[19] J. Stöhr, *NEXAFS Spectroscopy* (Springer, New York, 1992).
[20] C. Jacobsen, S. Wirick, G. Flynn and C. Zimba, J. Micros. 197 (2000) 173.
[21] A.P. Hitchcock, P. Hitchcock, C. Jacobson, C. Zimba, L.B.E. Rotenberg, J. Denlinger and R. Kneedler, aXis2000 – program available from http://unicorn.mcmaster.ca/aXis2000.html (1997).
[22] D.G.L. Sutherland, M. Kasrai, G.M. Bancroft, Z.F. Liu and K.H. Tan, Phys. Rev. B 48 (1993) 14989.
[23] Z. Yin, M. Kasrai, G.M. Bancroft, K. H. Tan and X. Feng, Phys. Rev. B. 51 (1995) 742.
[24] J.M. Martin, C. Grossiord, T. Le Mogne, S. Bec and A. Tonck, Trib. Int. 34 (2001) 523.
[25] ICP analyses were performed at the Sarnia Research Center at Imperial Oil Canada
[26] J.F. Graham, C. McCague and P.R. Norton, Trib. Lett. 6 (1999) 149.
[27] I.N. Koprinarov, A.P. Hitchcock, C.T. McCrory and R.F. Childs, J. Phys. Chem. B. 106 (2002) 5358.
[28] X. Zhang, R. Balhorn, J. Mazrimas and J. Kirz, J. Struct. Biol. 116 (1996) 335.
[29] M.N. Najman, M.Kasrai and G.M. Baner of wear (in press).
[30] F.G. Rounds, ASLE Trans. 30 (1987) 479.
[31] E.S. Yamaguchi, P.R. Ryason, E.Q. Labrador and T.P. Hansen, Trib. Trans. 39 (1996) 220.